

CHAPTER-6

Sedimentation in the Northeastern Arabian Sea: Implications to climate, tectonics and sea level

Indus sediment flux is the major source of sedimentation in the Arabian Sea which forms Indus submarine fan. The Indus submarine fan extends over 106 km² in the Arabian Sea with up to 9 km thick pile of sediments (Coumes and Kolla, 1984; Clift et al., 2001). An annual sediment discharge of about 450 x 10⁶ Tg.yr⁻¹ before damming (Milliman et al., 1984) representing the fifth largest sediment flux in the world (Bourget et al., 2013). The Indus River presently drains an area of approximately 10⁶ km² of the Himalayan region. The Indus River runoff mounts during the southwest monsoon season due to high precipitation and snow melting (Karim and Veizer, 2002). The drainage basin of the Indus River comprises high relief and poorly consolidated sediments, which is the major cause for the high sediment flux (Giosan et al., 2006) along with large runoff. Several studies during the last few decades to understand the evolution of Indus submarine fan (Bourget et al., 2013 and references therein). Clift and Giosan (2014) showed that a significant portion of the eroded sediment in the Indus drainage system is stored in the floodplains excluding the suspended loads. They also pronounced that the sedimentation in the Indus submarine fan lags erosion up to 10 ka B.P. Another study by Clift et al. (2014) has revealed that the sediment transfer from river mouth to submarine fan is primarily controlled by sediment mixing and reworking associated with sea-level changes. Thus, the relation of sedimentation in the Indus submarine fan and climate over the Indus drainage basin is very intricate. However, Bourget et al (2013) equated the late Quaternary sedimentation in Indus submarine fan with the sea level changes, and observed high sedimentation events occurred during low sea-level stands.

In this chapter, the sedimentation history of the Indus submarine fan has been reconstructed using 4016 sediment core data in comparison with the previously published datasets (Figure 6.1). The reconstructed sedimentation history has been matched with the palaeoclimate of the Indus drainage basin.

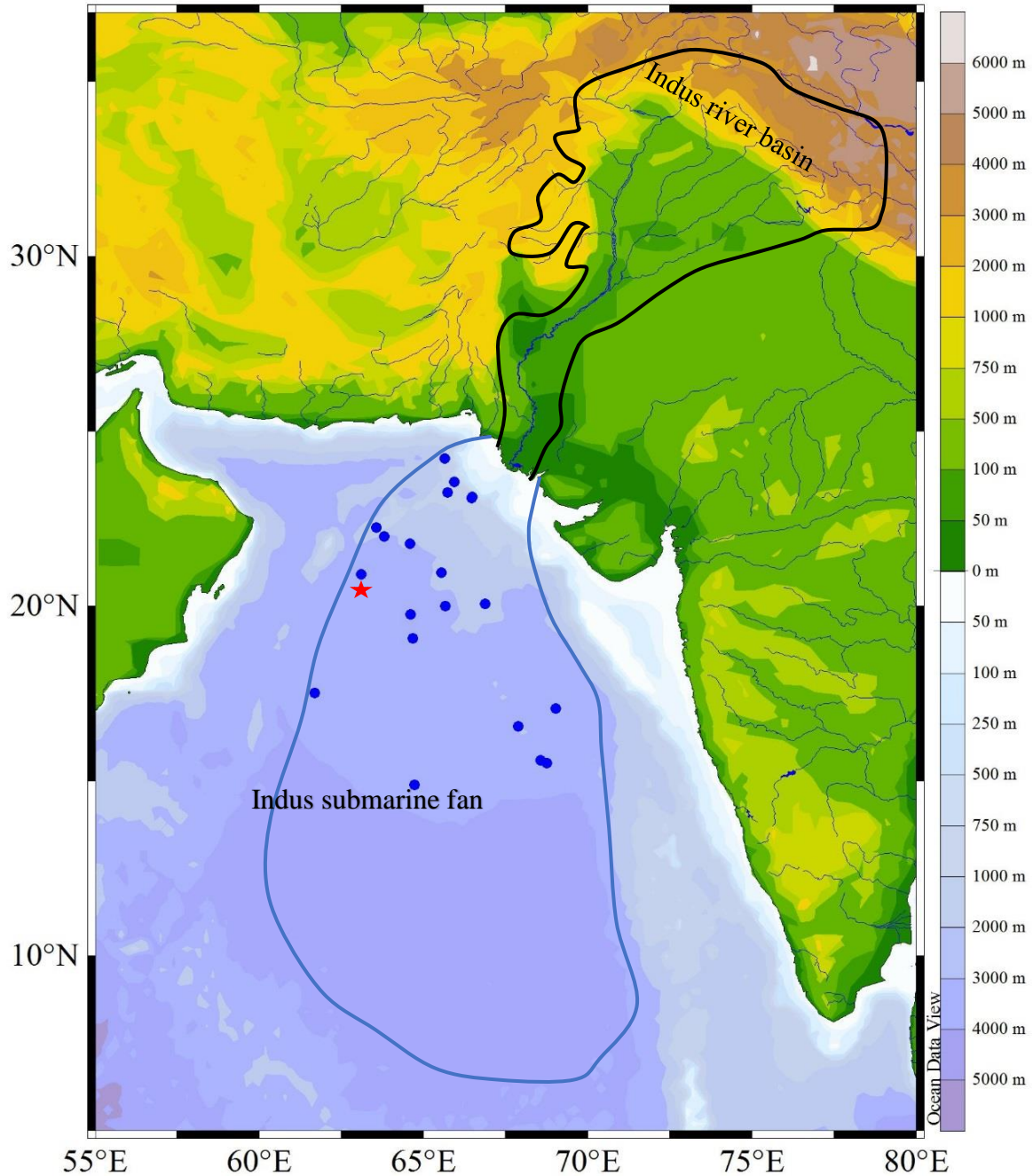


Figure 6.1: Map of the Indus River basin and submarine fan. Red star marks the location 4016 sediment core. Also shown are the locations of the previously published datasets (Sirocko, 1989; Reichart et al., 1998).

6.1 Results

6.1.1 Lithogenic Sediment accumulation Rate

The lithogenic sediment is a fraction of the marine sediment that is derived from the land to the oceanic basin. The lithogenic sediment flux primarily depends on the land erosion and transportation pathway. Numerous methods are employed to separate the lithogenic constituent from the marine sediments. One among those is the removal of major biogenic components (CaCO_3 , biogenic silica and organic carbon) from the bulk sediment (Rea, 1994). However, most marine basin have calcareous sediments, except high nutrient and upwelling regions where biogenic silica forms a significant proportion (Rea, 1994). Normally, in open ocean sediments, organic carbon content is less than 1 percent. In the present sediment core, the CaCO_3 content varies between 37 to 65 %, while, the concentration of organic carbon varies between 0.2 to 0.7 %. The non- CaCO_3 fraction of the sediment in the 4016 sediment core has been considered as lithogenic component. The mass accumulation rate has been calculated by multiplying the sedimentation rate with dry bulk density. The lithogenic sediment accumulation rate is the product of mass accumulation rate and lithogenic fraction.

The reconstructed lithogenic sediment accumulation rate varies between 4.8 to 22.5 $\text{g/m}^2/\text{yr}$ with a uni-modal distribution during the last 34.6 ka B.P. (Figure 6.2). The step like pattern in the flux record is caused by the influence of age control points and sedimentation rate. The lithogenic sediment flux is $\sim 12.3 \text{ g/m}^2/\text{yr}$ between 34.6 to 30 ka B.P. The lithogenic flux increased at 30 ka B.P. to a rate of $\sim 18 \text{ g/m}^2/\text{yr}$ and remained stable for a period of about 4 ka. From 26.4 to 23.2 ka B.P., the lithogenic flux remained at around $19 \text{ g/m}^2/\text{yr}$ with minor variations. The lithogenic sediment flux was highest ($\sim 21.6 \text{ g/m}^2/\text{yr}$) in the present core record through the period 23.2 to 20.5 ka B.P., after that it got reduced to around $18.8 \text{ g/m}^2/\text{yr}$ till 18.9 ka B.P. Marginal increase in the lithogenic sediment flux to $19.5 \text{ g/m}^2/\text{yr}$ has been observed between 18.9 to 17.3 ka B.P., and then it decreased to about $11.5 \text{ g/m}^2/\text{yr}$ between 17.3 to 14.4 ka B.P. The lithogenic flux again decreased at 14.4 ka B.P. to $\sim 10.5 \text{ g/m}^2/\text{yr}$ till 11.7 ka B.P. The last 11.7 ka period has been characterized by the lowest lithogenic flux (4.8 to $5.8 \text{ g/m}^2/\text{yr}$) in the present record.

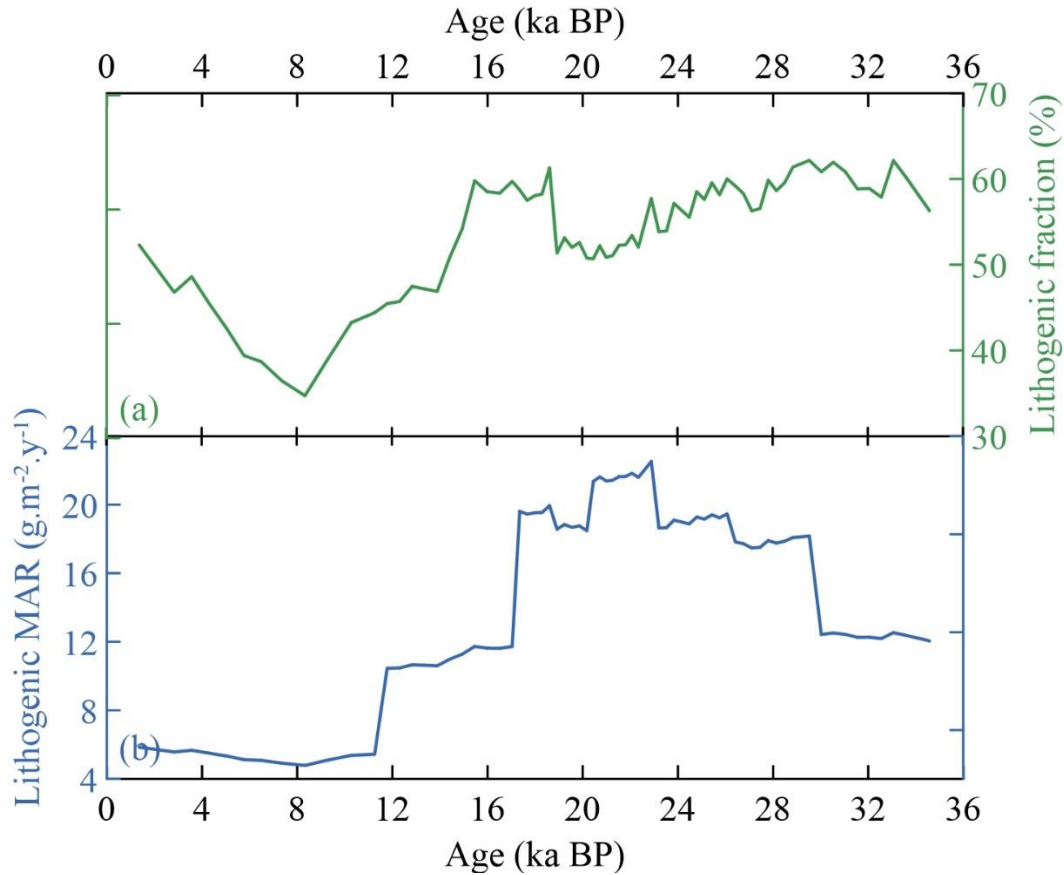


Figure 6.2: Lithogenic sediment fraction and flux in the 4016 sediment core record. (a) lithogenic sediment percentage, (b) lithogenic sediment mass accumulation rate.

6.1.2 Magnetic Susceptibility

Magnetic susceptibility measurements were carried out in all the samples of 4016 sediment core and were used to test the lithogenic sedimentation in marine environments. The variations in magnetic susceptibility data shows trend similar to that of lithogenic sediment fraction (non-CaCO₃ fraction) throughout the core record. The overall variation in the magnetic susceptibility during the last 34.6 ka B.P. has been observed between 1.74 and $3.08 \times 10^{-7} \text{ m}^3/\text{kg}$ (Figure 6.3). The magnetic susceptibility record depict five units of similar values during the last 34.6 ka B.P. The bottom most part of the record between 34.6 to 24.4 ka B.P. has magnetic susceptibility values more than $2.5 \times 10^{-7} \text{ m}^3/\text{kg}$. From 24.4 to 18.6 ka B.P., the magnetic susceptibility values decreased and remained between 2 to $2.3 \times 10^{-7} \text{ m}^3/\text{kg}$. After 18.6 ka B.P., the magnetic susceptibility values increased above $2.5 \times 10^{-7} \text{ m}^3/\text{kg}$ till 14.4 ka B.P., then later it continuously decreased to a minimum value of $1.7 \times 10^{-7} \text{ m}^3/\text{kg}$ at 8.3 ka B.P. The magnetic susceptibility

values of the sediments gradually increased during the last 8.3 ka B.P. in the present core record. The core top marks the highest magnetic susceptibility value in the last 34.6 ka B.P.

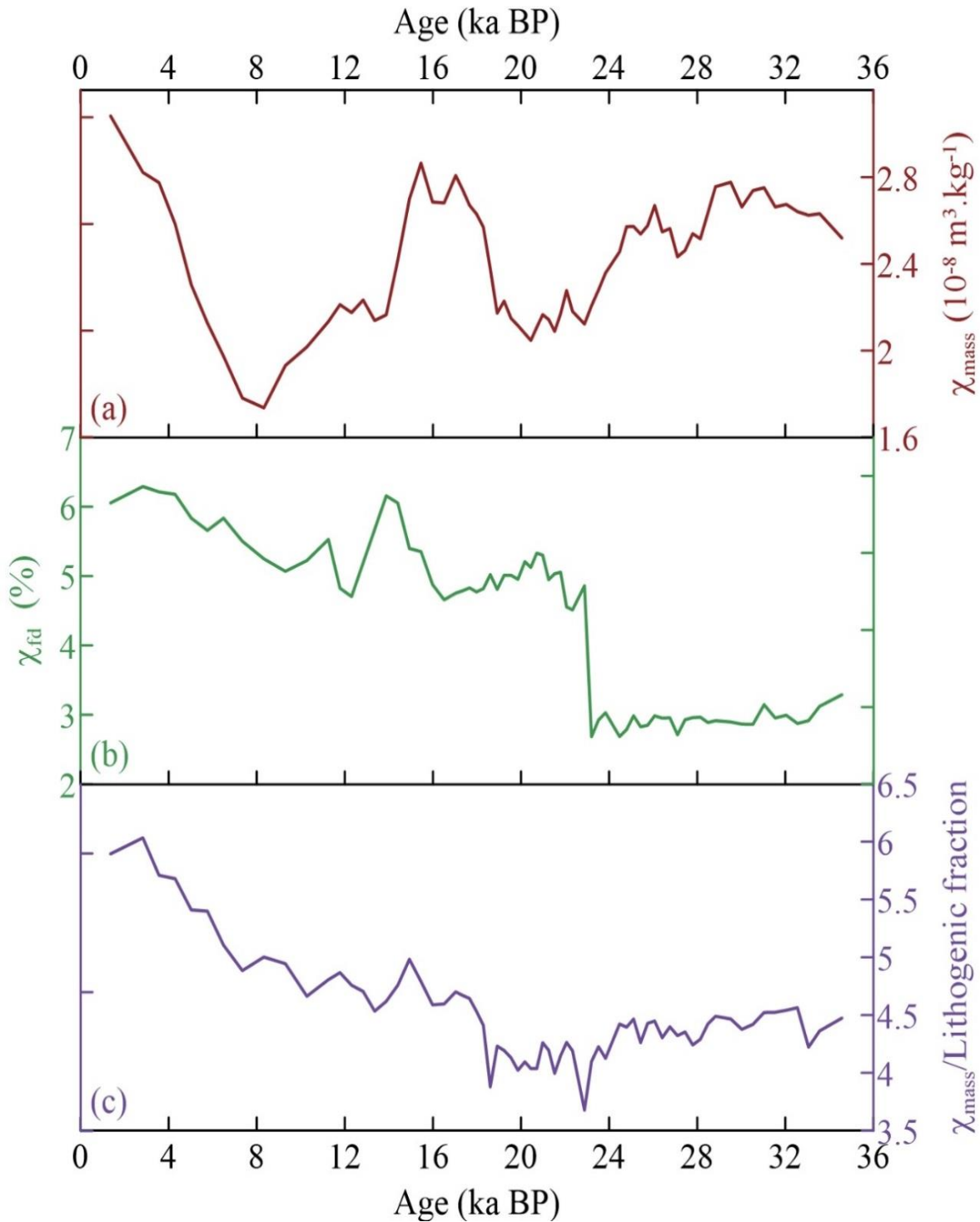


Figure 6.3: Magnetic susceptibility record of 4016 sediment core. (a) Magnetic susceptibility, (b) frequency dependent magnetic susceptibility, (c) magnetic susceptibility to lithogenic fraction ratio.

The frequency dependent magnetic susceptibility is a proxy for magnetic mineral grain size in the sediments. In the present record, the frequency dependent magnetic susceptibility varied between 2.7 to 6.3 %. It shows two set of values with a shift at around 23 ka B.P. The frequency dependent magnetic susceptibility has values less than 3.3 % between 34.6 to 23 ka B.P. However, it enhances more than 4.5 % in the last 23 ka B.P. with the maximum value at 2.8 ka B.P. The ratio between the magnetic susceptibility and lithogenic sediment fraction can provide some insight about the concentration of magnetic mineral in the lithogenic fraction of the sediments, and thereby changes in the source material. This ratio shows a moderate shift at 18.6 ka B.P., from a low towards an increasing trend.

6.1.3 Inorganic Geochemistry

Major lithogenic elements (Al, Ti, Fe and Mg) were measured in all the samples of the 4016 sediment core. The elemental concentration are represented on carbonate free basis (cfb) in Figure 6.4. The use of Ti over Al is favoured by many recent studies is due to non lithogenic contribution of Al (van Bennekom et al., 1989; Murray et al., 1993; Murray and Leinen, 1996; Dixit et al., 2001). Elemental concentration in the cfb fraction did not show any significant change during the last 34.6 ka B.P. However, there are short term changes in the concentration and ratio.

The Al concentration varied between 5.7 to 9.2 % during the last 34.6 ka B.P. The Al concentration remained similar both at top and bottom of the sediment core (Figure 6.4a). The Al concentration was around 7 % between 34.6 to 28 ka B.P., then it increased to 8 % and remained till 19 ka B.P. From 19 to 13 ka B.P., a drastic change in the concentration high and low is observed. During the last 13 ka B.P., the Al concentration has gradually decreased. The Al/Ti ratio show a totally different scenario with an abrupt shift at 26 ka B.P. (Figure 6.4 a). The Al/Ti ratio was above 20 between 34.6 to 26 ka B.P., which lowered to 18 and remained more or less stable during the last 26 ka B.P. The Ti concentration in the present sediment core ranged between 0.3 to 0.53 % (Figure 6.4 b). There were two set of values observed with around 30% variation between them. The lower concentration has been observed between 34.6 and 26 ka B.P, and the high concentrations were observed during the last 26 ka B.P. However, the overall variation of the Ti concentration has a narrow range.

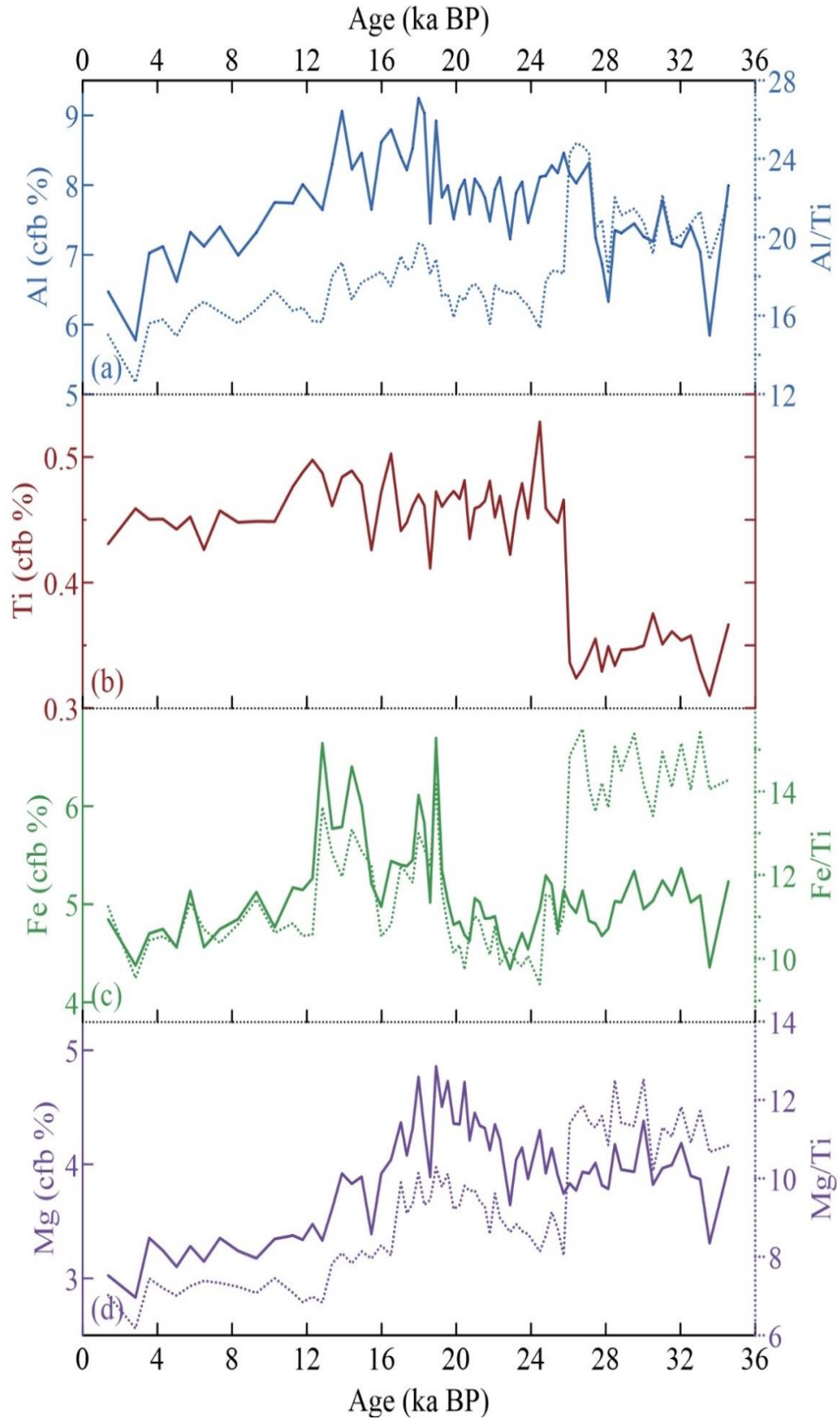


Figure 6.4: Variation of major element concentration with age and its ratio to Ti in the sediment core 4016 in the northern Arabian Sea.

The Fe concentration varied between 4.3 to 6.7 % in the present record (Figure 6.4c). Except the period between 19.5 to 11.7 ka B.P., the Fe concentration has remained ≤ 5 %. During 19.5 to 11.7 ka B.P., the Fe concentration in the sediment samples stayed above 5 %. The Fe/Ti ratio has a pattern similar to Al/ Ti with an abrupt shift at 26 ka B.P. (Figure 6.4c). However, increased values of Fe/Ti were also recorded between 19.5 to 11.7 ka B.P. The Mg concentration has three range of values during the last 34.6 ka B.P. (Figure 6.4d). The high concentration of Mg has been observed between 24 to 16 ka B.P., while the lowest concentration during the last 16 ka B.P. The period between 34.6 to 24 ka B.P. was characterized with intermediate Mg concentrations.

6.2 Discussion

6.2.1 Lithogenic Sedimentation in the Indus Fan

Lithogenic sedimentation in the Indus submarine fan has been reconstructed using the present sediment core data along with previously published data sets (Sirocko, 1989; Reichert et al., 1998). All the previously published datasets were corrected for the CaCO₃ concentration and the lithogenic sediment flux were estimated with a similar procedure discussed earlier. Since the sampling were unevenly spaced in time, time averaged slices were calculated for each sediment core. The time slices were based on the change in timing of the lithogenic sediment flux in 4016 sediment core. Averaged lithogenic sediment flux were calculated for 34 to 29 ka B.P., 29 to 26 ka B.P., 26 to 17 ka B.P., 17 to 11.7 ka B.P. and 11.7 to 0 ka B.P. Contour mapping of each time slice were created in Ocean Data Viewer (ODV version 4.3.10) using linear interpolation method. The contour maps for each time slice depicts the sedimentation variations over space and time. In all the five time slices, the highest lithogenic sedimentation was observed near the river mouth as expected which decreases off the coast. This is due to the reduction of sediment carrying capacity by the river losses from the river mouth to the open ocean.

The lithogenic sedimentation was higher during the period 34 to 29 ka B.P. The sediment distribution was asymmetric with southern part having higher sediment flux than northern part of the river mouth. This suggests that there was an influence of clockwise surface currents in the study area during 34 to 29 ka B.P. leading to enhanced sedimentation in the southern part. The secondary sedimentation maxima at 20° N also indicates the persistent influence of dust flux in the distal fan sedimentation.

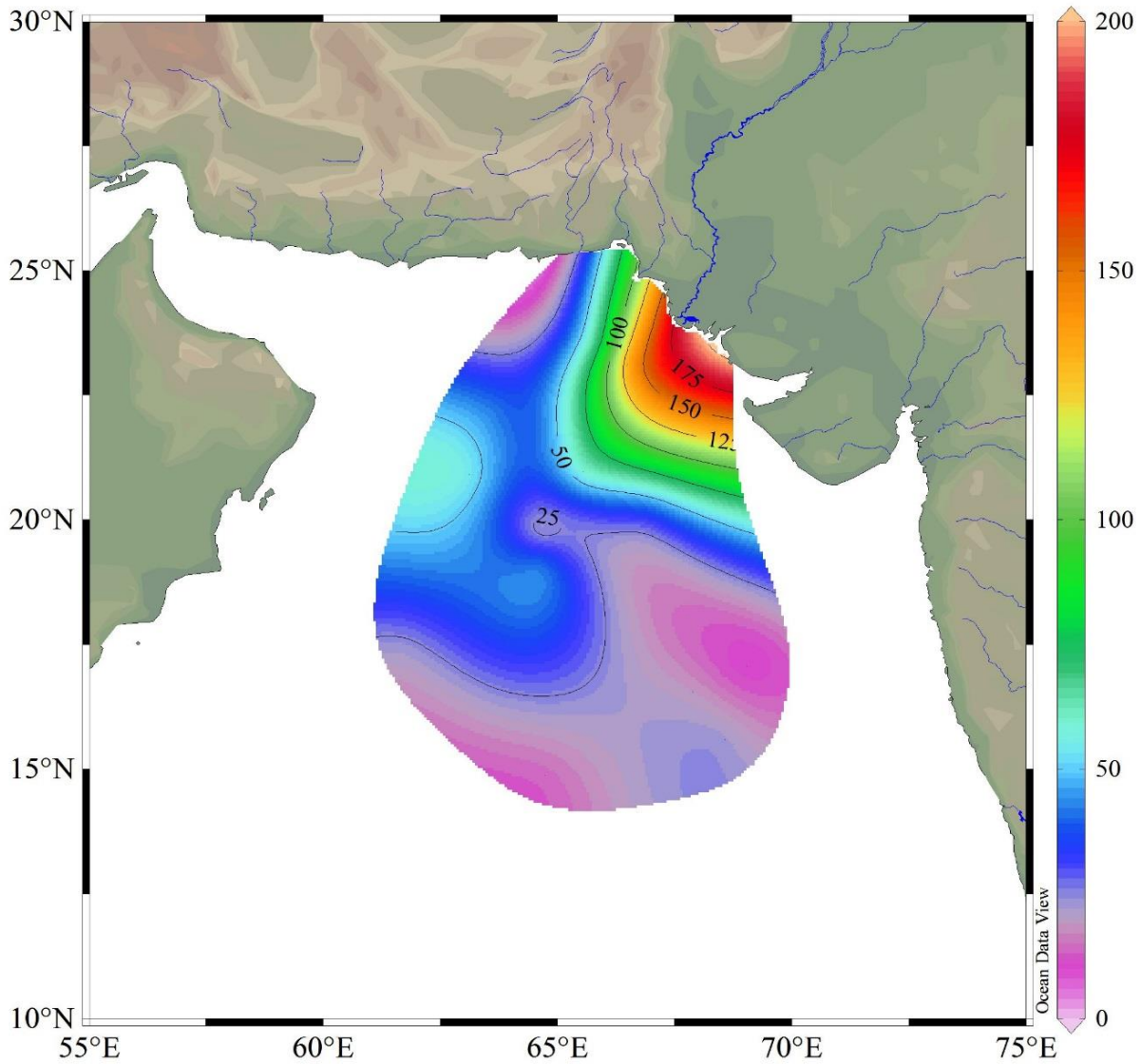


Figure 6.5: Average lithogenic sediment flux ($\text{g/m}^2/\text{y}$) during 34 to 29 ka B.P. from Indus River in the northern Arabian Sea.

The average lithogenic sediment flux during 29 to 26 ka B.P. was comparatively lower than during the period 34 to 29 ka B.P. The asymmetric distribution of sedimentation towards southern side of the river mouth suggests clockwise surface circulation. The surface circulation indicates the presence of southwest monsoonal winds, but with reduced sediment flux from Indus River. The secondary sedimentation maxima which also occurred during this period indicates the influence of dust flux.

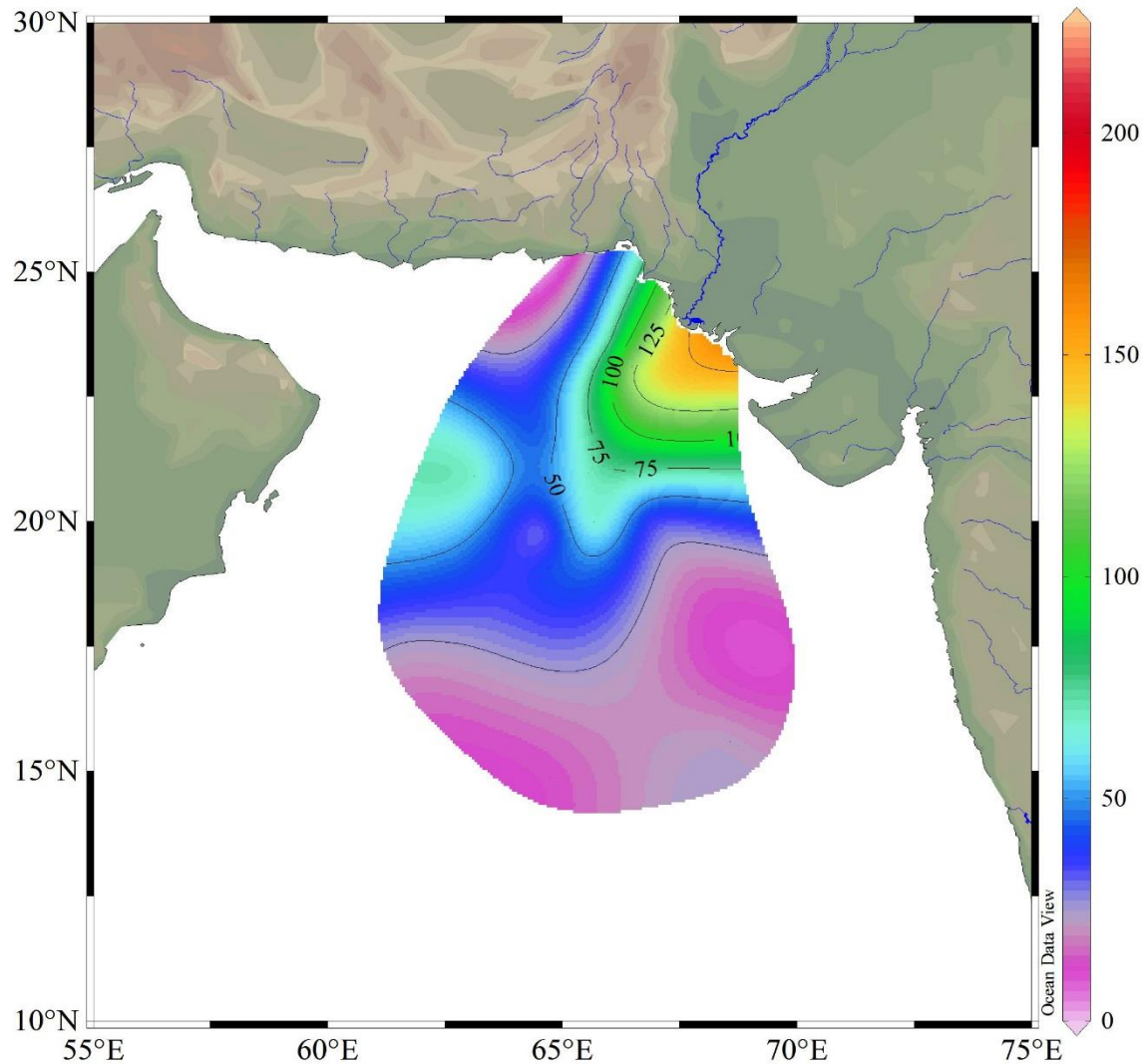


Figure 6.6: Average lithogenic sediment flux ($\text{g/m}^2/\text{y}$) during 29 to 26 ka B.P. from the Indus River in the northern Arabian Sea.

The average lithogenic sediment flux during 26 to 17 ka B.P. (Figure 6.7) shows that the sedimentation maxima occurred near the coast as expected. However, the maximum sedimentation occurred on the northern part of the river mouth. This indicates alteration in sediment redistribution thereby the change in surface current direction. In the modern scenario, the surface current flows counter-clockwise during the northeast monsoon season and redistributes the Indus derived sediments towards north. The sedimentation pattern during the period 26 to 17 ka B.P. matches with the northeast monsoon surface circulation pattern. Thus, northward distribution of sediment during this period could be due to strengthening of the northeast monsoon. Additionally, there

seems to be a secondary sedimentation maxima near the mid-west part of the submarine fan near 20° N. This secondary sedimentation maxima can be attributed to the dust flux from Arabian Desert as the region locates in the direction of dust trajectory at modern times.

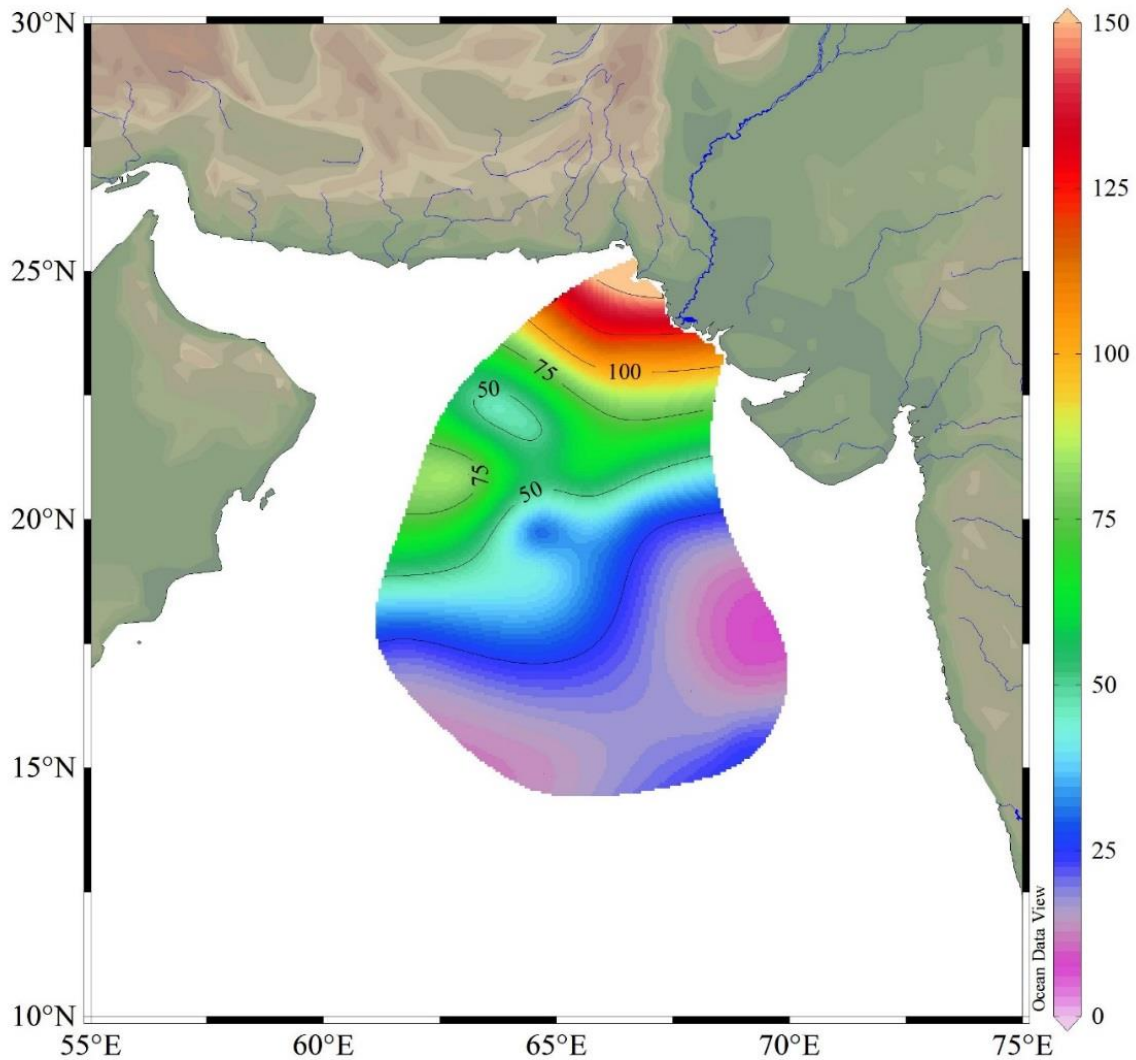


Figure 6.7: Average lithogenic sediment flux ($\text{g/m}^2/\text{y}$) during 26 to 17 ka B.P. from the Indus River in the northern Arabian Sea.

It is however suggested that the sedimentation was low during 26-17 ka B.P. and the lithogenic sedimentation increased in the distal region of Indus submarine fan, which is the case with 4016 sediment core. This could be due to the mixing of sediment from different sources. The sources of sediments for the distal fan region could have been Indus derived, dust flux and sediments from the peninsular rivers. However, the idea of re-deposition of older sediments have

been ruled out due to the fact that the chronology of 4016 sediment core is continuous with no reversal or abrupt variations. The peninsular river sediments can be brought to the submarine fan region by the counter-clockwise circulation of surface current prevailed during this period. The dust flux might have increased due to the intense aridity that occurred during LGM period. Therefore the use of distal fan sediments for reconstructing the changes in drainage basin during the LGM period must be done with due consideration with the sediment mixing.

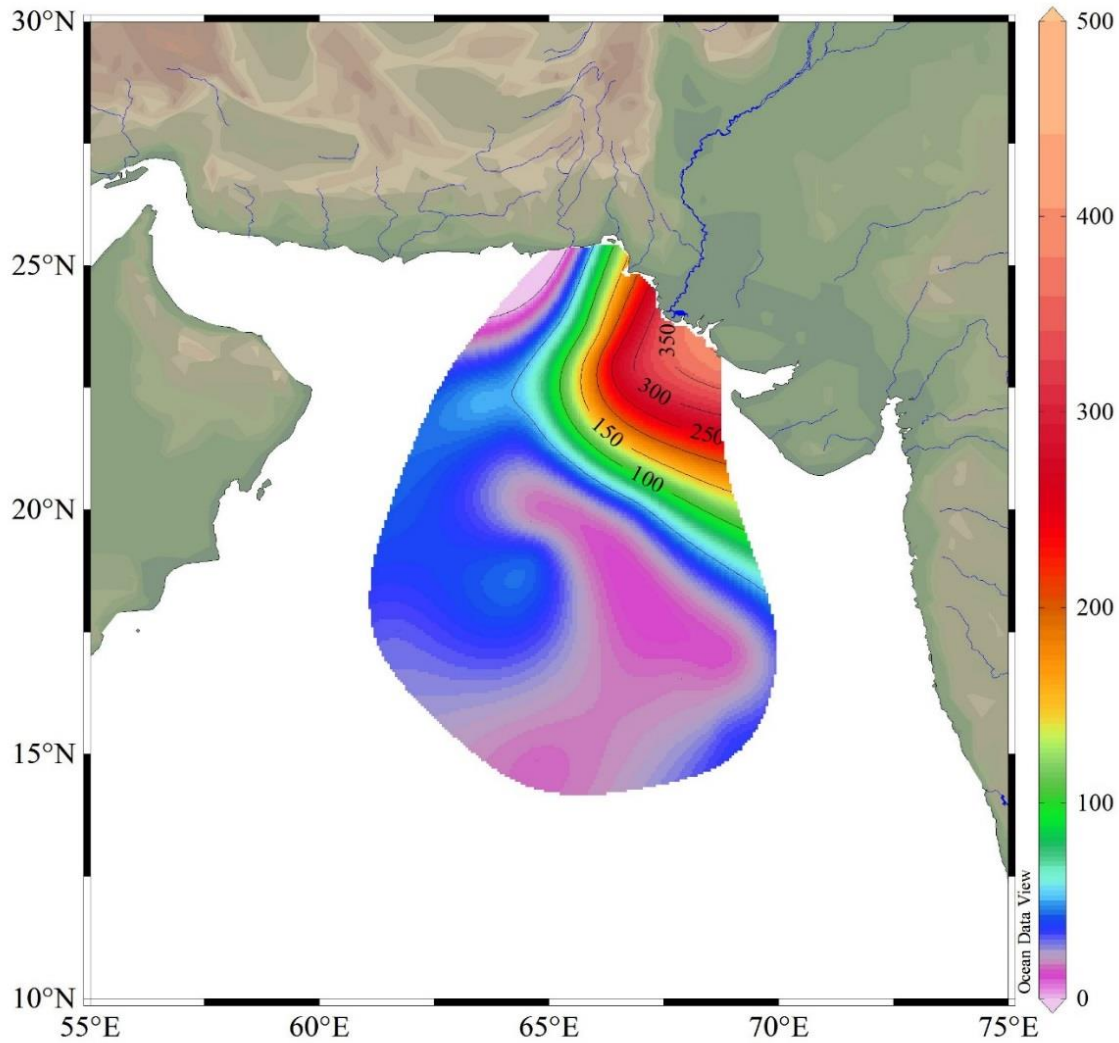


Figure 6.8: Average lithogenic sediment flux ($\text{g}/\text{m}^2/\text{y}$) during 17 to 11.7 ka B.P. from the Indus River in the northern Arabian Sea. The sediment flux is more than two times higher than recent sedimentation.

During the time slice 17 to 11.7 ka B. P. it appears that the sedimentation was much higher. Not only the lithogenic sediment flux increased, but also the asymmetric nature of sediment

deposition on either side of river mouth. This indicates stronger clockwise surface currents during this time thereby stronger southwest monsoon. Previous studies from other part of the basin indicated strengthened southwest monsoon during early Holocene (11.7 to 9 ka B.P.) (Tiwari et al., 2010). The present dataset however indicates strengthened southwest monsoonal surface currents during deglacial period (17 to 11.7 ka B.P.). The sediment flux depends on many factors, the slope gradient, water discharge volume, sediment nature and availability. All other parameters being constant, the high sediment flux during the deglacial period could have been caused by the increased southwest monsoon along with glacial retreat.

The high sedimentation during 17 to 11.7 to ka B.P. occurs near the coast as well as in the deep submarine fan indicating the massive sediment load debouched by the Indus River. However, marginally higher sedimentation in the southwestern part of the study area indicates probable influence of aeolian sediment supply to the northern Arabian Sea during the deglacial period from Arabian Deserts. The increased Mg concentration during the deglacial period in the 4016 sediment core confirms the above interpretation that the Arabian dust flux has increased during deglacial period. The Fe as well as magnetic susceptibility records also show an increase during the deglacial period.

The average lithogenic sediment flux for the last 11.7 ka B.P. is shown in Figure 6.9. Note, the highest sediment flux near the river mouth. However, the maximum flux occurs at the southern part of the river mouth, making an asymmetric distribution of sediment. At present, the maximum sediment flux occurs during the southwest monsoon season. The clockwise surface currents might have redistributed the sediment load towards the southern part making maximum sedimentation in southern part of the river mouth.

Overall, it has been interpreted from the sedimentation pattern in the Indus submarine fan that the Indus derived sediments undergo reworking by surface water currents and get mixed with other sediments. Most of the sediments derived from the Indus River during the last 34 ka B.P. was distributed southwards due to clockwise currents, except during LGM when the sediments were transported towards north by counter-clockwise surface currents. Though the 4016 sediment core record has highest sedimentation during the LGM (Figure 6.2), the overall pattern shows the maximum lithogenic flux occurred during the deglacial period (Figure 6.8). This could have been

caused by the fall in sea level and decreased storage capacity of the shelf region. The influence of other sediment sources like Arabian dust and peninsular river sediments were mostly confined to the north-western and south-eastern part of the Indus submarine fan.

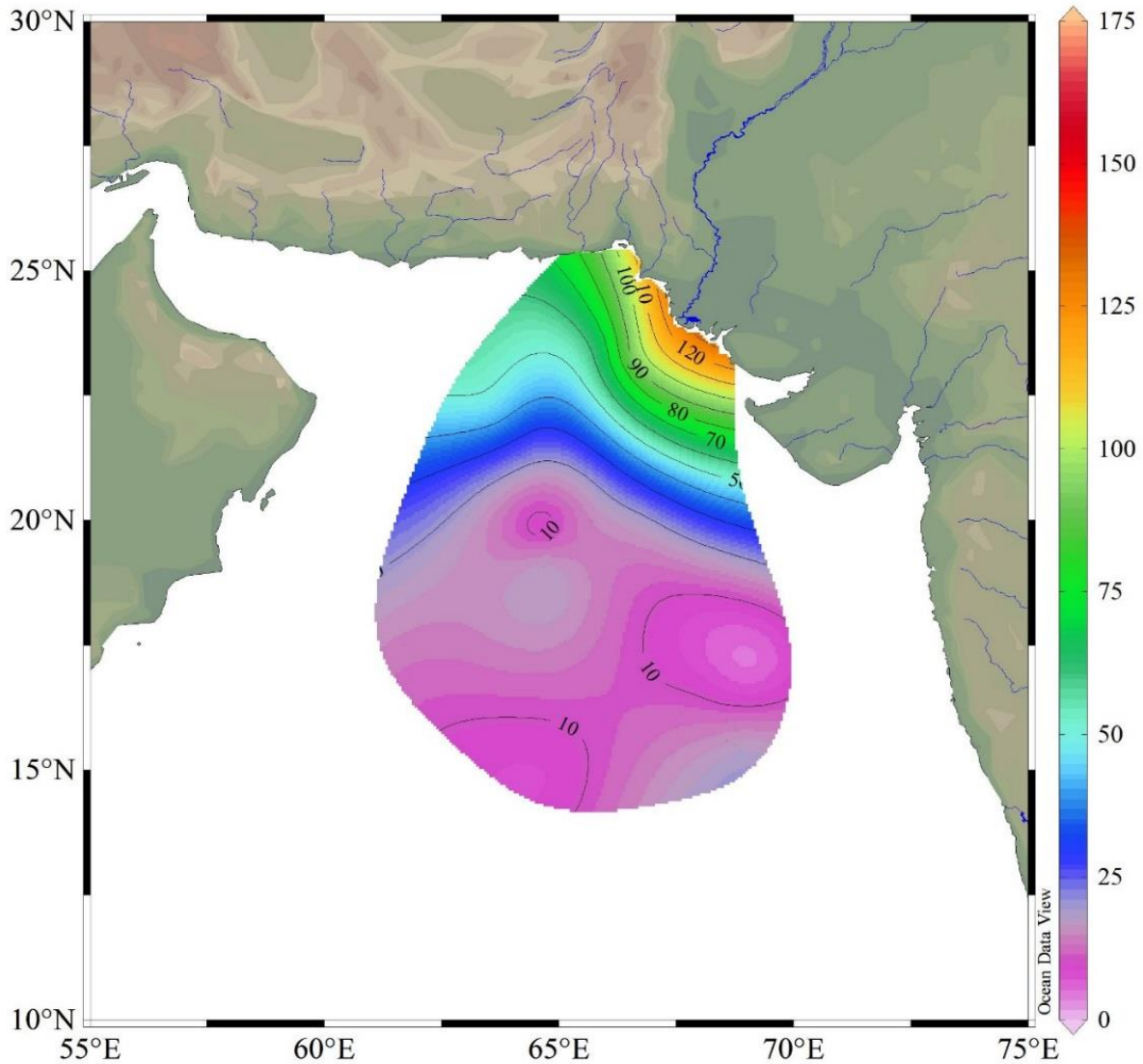


Figure 6.9: Average lithogenic sediment flux ($\text{g}/\text{m}^2/\text{y}$) from the Indus River during the last 11.7 ka B.P.

6.2.2 Sea Level and Sedimentation

Lithogenic sediment flux variations due to sea level fluctuation is dependent on the location. The reduced sea level can increase sedimentation in the deeper part of the basin like lower

shelf and slope, while reduced sedimentation can be observed in the upper shelf region due to loss of storage capacity (Clift and Giosan, 2014). The reduced sea level also leads to increase in the stream energy and sediment carrying capacity due to change in the slope gradient. On the other hand, the increase in sea level can rather be opposite and would increase the sedimentation near the coast/upper shelf due to the increase in storage capacity. The sediment flux alone can change the local sea level by altering the coastal geometry.

Here, the lithogenic sediment flux has been compared with the global sea level fluctuations to understand how the sea level influenced the sedimentation during the last 34.6 ka B.P. (Figure 6.10). The lithogenic sediment flux in the present core record (4016) shows an inverse relation with the sea level, high sediment flux during low sea level and vice versa. The inverse relation clearly indicates that the sedimentation in the 4016 core region is significantly influenced by the variation in mean sea level. The sea level during the time period between 34.6 to 29 ka B.P. was nearly stable, lower than present and higher than LGM. The sediment flux was also moderate during this period. From 29 ka B.P., the sea level regressed, while in the meantime the lithogenic sediment flux increased. The decreasing sea level reduced the storage capacity for sediment deposition in the shelf region and increased the sediment supply towards deeper parts of the submarine fan. This process was again accelerated during the LGM period (26 to 17 ka B.P.) by the lowest sea level.

Highest lithogenic sediment flux was observed during the LGM in the 4016 sediment record. After the LGM, the sea level again increased during 17 to 11.7 ka B.P., while the lithogenic sediment flux decreased by the production of more storage capacity in the shelf region. However the average lithogenic sediment flux in the basin increased during 17 to 11.7 ka B.P. (Figure 6.10 box plot). The increasing pattern in the average sediment flux were mainly caused by the near coastal records. During the last 11.7 ka B.P., the sea level increased again and reached present day sea level, while the lithogenic sediment flux decreased to its lowest rate. The 4016 record as well as the previously published record show similar reduction in lithogenic sediment flux during the last 11.7 ka B.P. Overall, it has been observed that the variation in sea level had significant control on the lithogenic sediment flux to the Indus submarine fan throughout the last 34.6 ka B.P.

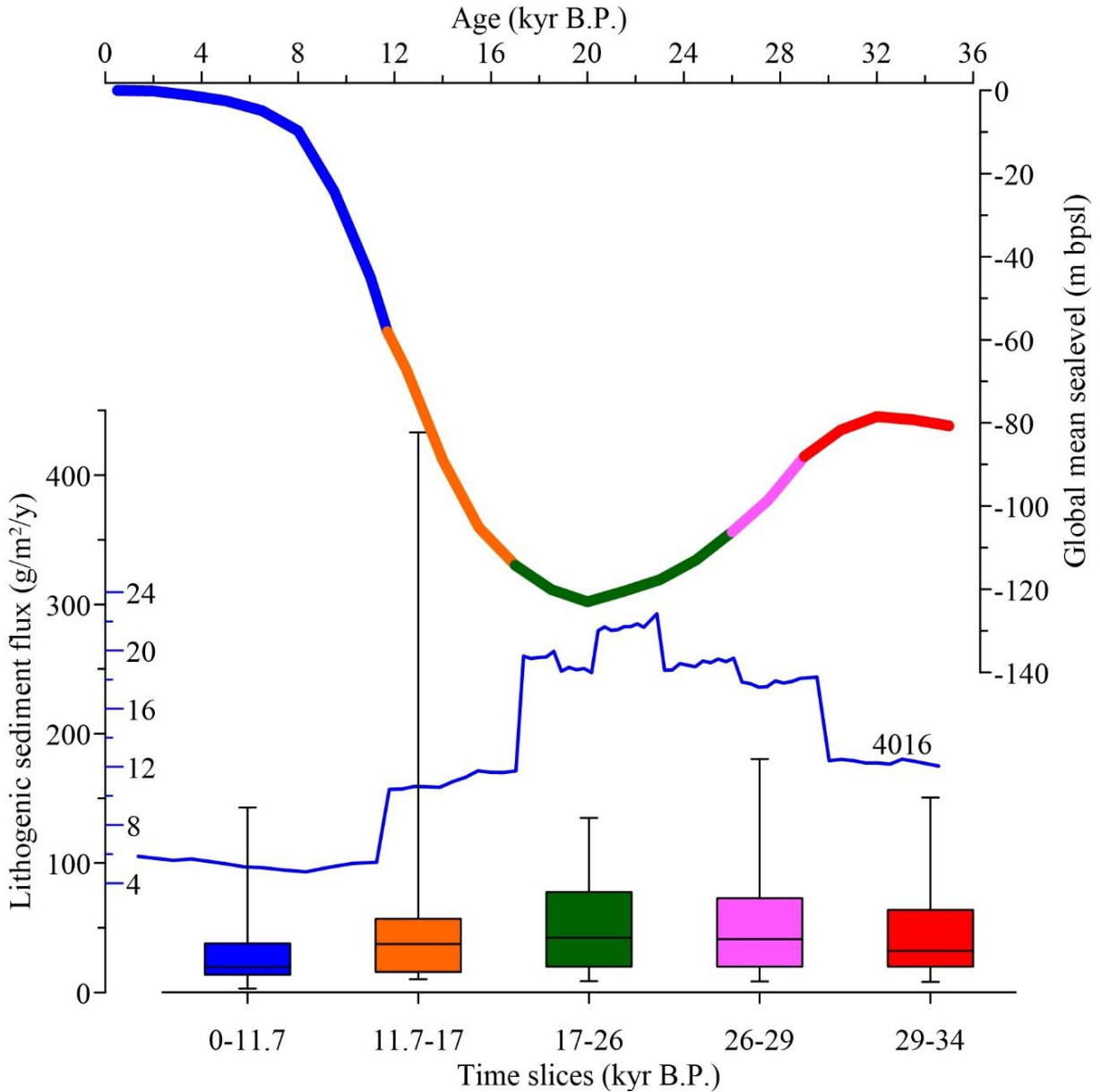


Figure 6.10: Comparison of lithogenic sediment flux in the Indus submarine fan with global sea level curve (meters below present sea level; Waelbroeck et al., 2002). Box plot shows the average lithogenic sediment flux during each time slices.

6.2.3 Himalayan Climate vs Lithogenic Flux

Climate in general and precipitation in particular have had significant impact on the river energy to erode and transport the sediment from the mountain region. Theoretically, the precipitation in drainage basin would have forward relation with the sediment flux to the depocentre or depositional basin. The transfer of the precipitation signal to the basin in the form

of sediment flux may not be quicker (annual or decadal time scales) due to the sediment deposition in the alluvial plains. However, the long-term changes in the environmental condition would eventually get transferred to the basin. In addition to the precipitation, glacier advance and retreat can influence the river runoff by altering the fresh water input. It can also modify the erosion and sediment discharge by changing the erodible area in mountain region. Dadson and Church (2005) showed that the high sediment transport by fluvial system occurs for longer period after the retreat of ice. The precipitation and glacier dynamics together can significantly influence the sediment discharge in a fluvial system like Indus. To understand the source to sink transfer of climate signal in the Indus River system, the submarine fan sedimentation record has been compared with the Himalayan climate record. Figure 6.11 shows the comparison between average sedimentation in Indus submarine fan, sediment flux in 4016 record and Guliya ice cap $\delta^{18}\text{O}$ record. The depleted oxygen isotope value in Guliya ice cap record indicates cold phase with weakened southwest monsoon precipitation and strong westerlies, while the enriched values indicate the opposite (warm phase with strengthened southwest monsoon precipitation and weak westerlies).

The comparison of Himalayan climate with Indus submarine fan sedimentation shows an interesting relation. The high sediment flux was recorded during cold and weak monsoon period (29-26 and 26-17 ka B.P.), but low sediment flux is observed during warm and strengthened monsoon period (last 11.7 and 34.6 to 29 ka B.P.). This negative relation between the Himalayan climate and Indus fan sedimentation is not expected. However, there are other possible reasons that could have caused the negative relation. It can be caused by the mask effect of sea level influence on sedimentation, means that the climate may have had a positive relation, but the stronger influence of sea level masked it. Other possible reason for the high sediment flux during weak monsoon phase might be the ice cover. Phillips et al. (2000) observed that the western Himalayan region experienced no major advance in ice cover during LGM, instead more ice cover could be observed during warm monsoonal phase like early Holocene. The less ice cover could have exposed the glacier eroded sediments and the melting might have caused more sediment discharge during LGM. The extended ice cover during warm monsoonal phase might have caused the opposite. However, the relation is more complex and could not be explained with the present dataset.

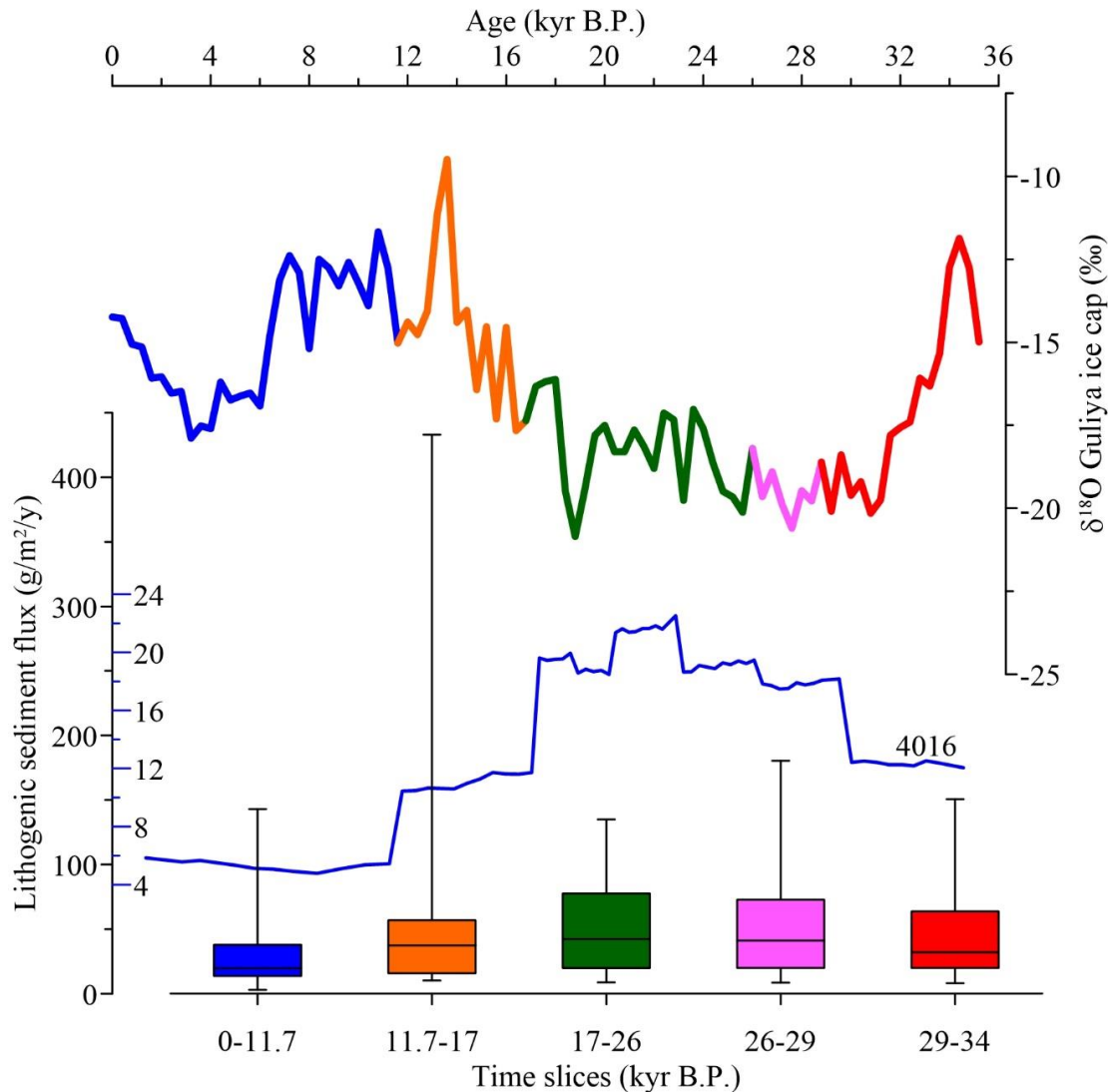


Figure 6.11: Comparison of Indus submarine fan sedimentation with western Himalayan climate (Guliya ice cap data; Thompson et al., 1997).

6.2.4 Himalayan tectonics vs Lithogenic Flux

The uplift of the mountain region has much larger control on the physical erosion and subsequent transport of sediment by the rivers flowing through that terrain. The uplift of bedrock accelerates the river incision in the mountain region. Dating the incised river terraces can give us the palaeo-incision rate for a particular time span. There are several palaeo-incision studies in the Indus River basin during the last two decades (Burbank et al., 1996; Thakur et al., 2014; Dey et al., 2016 and reference therein). The palaeo-incision rates were compared with the sedimentation in the Indus submarine fan to assess the first order relationship between them. Here, it is also assumed that the uplift/incision signal gets transferred to the basin on longer time scales. However,

the sedimentation in the alluvial plains should not be omitted. Also, the influence of sea level on sedimentation may have control on the relation between the variables discussed here.

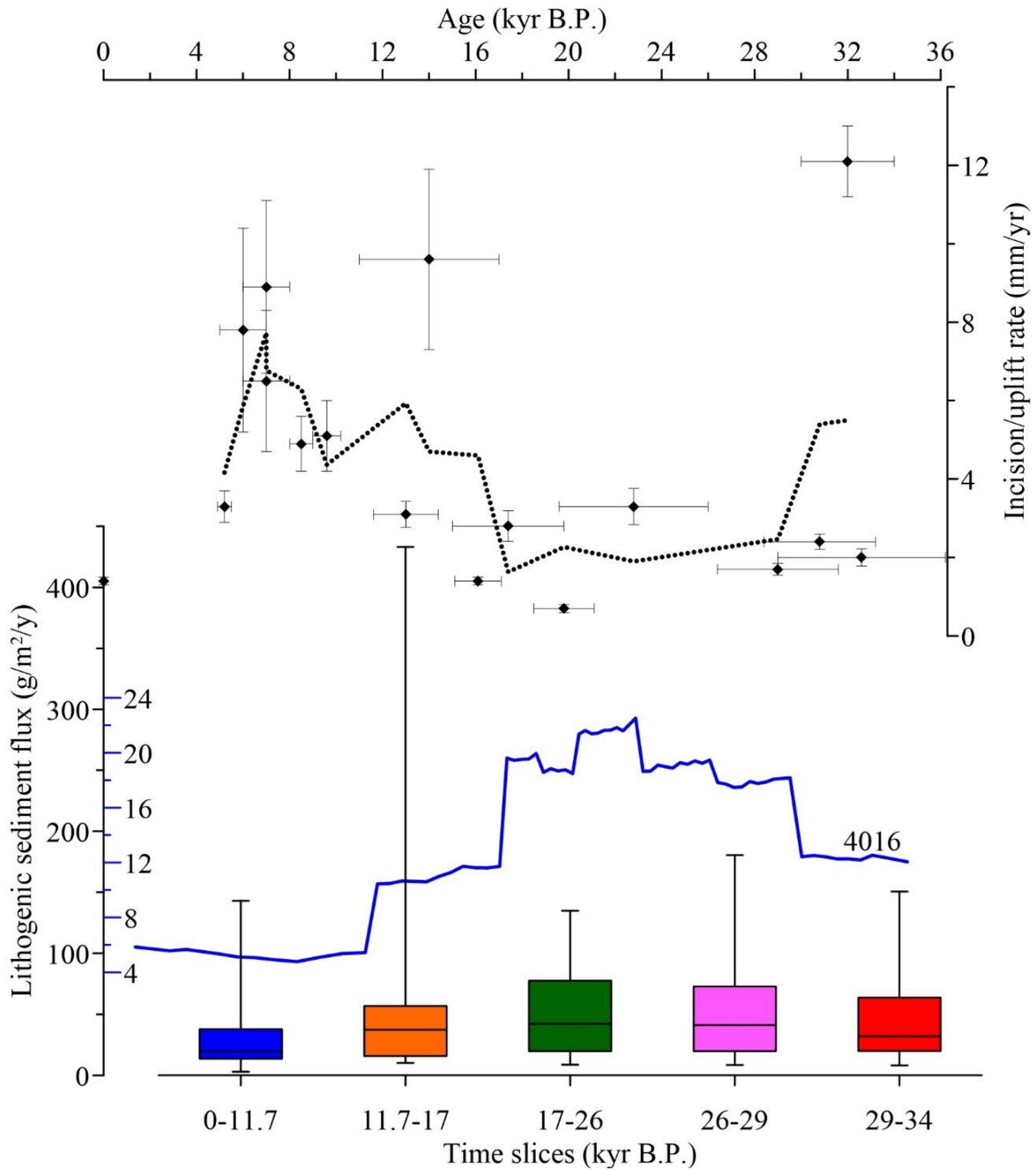


Figure 6.12: Comparison of palaeo-uplift/incision rate in the northwestern Himalaya (Indus River basin, Burbank et al., 1996; Thakur et al., 2014; Dey et al., 2016) with sediment flux in the Indus submarine fan. The dotted line shows the three point average. Blue line is the sediment flux rate in 4016 sediment core and the box plot shows the average sediment flux in the Indus submarine fan.

The relation between the Himalayan tectonics and Indus submarine fan sedimentation shows that the high incision rates are correlatable with low sedimentation and vice versa. Highest incision rates were recorded around 14 and 6 ka B.P., while the lowest incision rates were observed during LGM and during modern period. However, the highest lithogenic sediment flux to the Indus submarine fan was recorded during the LGM. Aggradation in the fluvial plains might be the possible reason for the low sedimentation during the high incision periods. But the erosion of fluvial plain deposits caused by lowered sea level can be a reason for the high sediment flux during LGM. Therefore, a detailed study on the fluvial plain deposition would be necessary before making any conclusive statement on the relation between the western Himalayan tectonics and the Indus submarine fan sedimentation.